ChemCatChem

Research Article
doi.org/10.1002/cctc.202402096

Chemistry Europe
European Chemical Societies Publishing

www.chemcatchem.org

In-Pt Supported Catalytically Active Liquid Metal Solutions for Propane Dehydrogenation – Role of Surface Acidity of Support

Moritz Wolf,[a, b] Thomas Gradl,[c] Shaine Raseale,[d] Aleksandr Maliugin,[a] Narayanan Raman,[c] Patrick Schühle,[c] Nicola Taccardi,[c] Michael Claeys,[d] Dmitry I. Sharapa,[a] Felix Studt,[a, e] Nico Fischer,[d] Marco Haumann,[c] and Peter Wasserscheid*[c, f]

Propane dehydrogenation is a dynamic catalytic application associated with rapid deactivation due to coking. Supported catalytically active liquid metal solutions (SCALMS) have been demonstrated to suppress coking due to the highly dynamic active sites at the liquid metal–gas interface. Herein, the parent catalysts for In-Pt SCALMS were prepared by impregnation using a series of alumina supports with various surface acidity. Reduction in hydrogen results in the formation of a supported liquid In-rich alloy, which was studied using in situ X-ray diffraction. The concentration profile of Pt is modeled via machine learning force field molecular dynamics simulation confirming an enrichment of Pt below the surface of the liquid alloy. The SCALMS with the least acidic alumina support results in a superior performance during propane dehydrogenation. In situ high-resolution thermogravimetric analysis coupled with mass spectrometry indicates enhanced coking with increasing alumina acidity, while comparison with a Pt/Al_2O_3-supported catalyst highlights the coking resistance of SCALMS.

1. Introduction

Light olefins are primary building blocks and basic compounds in the chemical industry due to the associated reactivity of the C—C double bond.[1–5] Demand for propylene has particularly increased in recent years, bringing more selective processes into focus. The direct catalytic dehydrogenation of propane to propylene (Equation 1) represents great potential enabling higher yields than steam or catalytic cracking, but requires a concentrated propane feed.[1–3,5]

$$C_3H_8 \rightleftarrows C_3H_6 + H_2 \quad (1)$$

Propane dehydrogenation (PDH) is a strongly endothermic reaction requiring elevated operation temperatures.[2] Undesirable side reactions, such as isomerization, hydrogenolysis, and cracking, are accelerated alongside increased temperatures >500 °C promoting the formation of coke. Pt/γ-Al_2O_3 and CrO_x/γ-Al_2O_3 catalysts are used in the industry. The γ-Al_2O_3 supports provide the required high surface area enabling high dispersion of the metal species and, in particular, a high mechanical stability of the catalysts. The addition of promoters, such as Sn, enhances the catalytic properties of the catalysts in many ways. For example, Sn suppresses side reactions by neutralization of acidic surface sites on γ-Al_2O_3.[2] Aside from introducing electronic synergies, secondary metals are often used in PDH to enhance the catalytic activity via ensemble effects or a reduced susceptibility for coking. Incorporation of Sn has been reported to reduce Pt nanoparticle size increasing the dispersion of the active phase. Further, the literature suggests a structural dependency of the coke formation over such bimetallic species,[6–8] which is generally accepted to be the culprit for the rapid catalyst decay.[9–12] In contrast, catalytic dehydrogenation is believed to be a structure-insensitive reaction and can be catalyzed by small clusters or even single atoms in high efficiency. Hence, single-atom or single-atom-alloy Pt catalysts, as well as catalyst concepts exhibiting a high coke resistance during PDH are at the focus of recent studies.[10,11,13–15]

Recently, we presented the promising catalyst concept of supported catalytically active liquid metal solutions (SCALMS)

[a] M. Wolf, A. Maliugin, D. I. Sharapa, F. Studt
Karlsruhe Institute of Technology (KIT), Institute of Catalysis Research and Technology, Hermann-von-Helmholtz-Platz 1, 76344, Eggenstein-Leopoldshafen, Germany

[b] M. Wolf
Karlsruhe Institute of Technology (KIT), Engler-Bunte-Institut, Engler-Bunte-Ring 3, 76131, Karlsruhe, Germany

[c] T. Gradl, N. Raman, P. Schühle, N. Taccardi, M. Haumann, P. Wasserscheid
Friedrich-Alexander-Universität Erlangen-Nürnberg (FAU), Lehrstuhl für Chemische Reaktionstechnik (CRT), Egerlandstr. 3, 91058, Erlangen, Germany
E-mail: peter.wasserscheid@fau.de

[d] S. Raseale, M. Claeys, N. Fischer
University of Cape Town (UCT), Catalysis Institute, Private Bag X3,, Rondebosch 7701, South Africa

[e] F. Studt
Karlsruhe Institute of Technology (KIT), Institute for Chemical Technology and Polymer Chemistry, Engesserstr. 18, 76131, Karlsruhe, Germany

[f] P. Wasserscheid
Forschungszentrum Jülich, Helmholtz Institute Erlangen-Nürnberg for Renewable Energy (IEK 11), Cauerstr. 1, 91058, Erlangen, Germany

Supporting information for this article is available on the WWW under https://doi.org/10.1002/cctc.202402096

combining single-atom catalysis with coke resistance.[13,14,16–18] The concept represents a subcategory of supported liquid phase (SLP) catalysts that combine advantages from homogeneous and heterogeneous catalysis.[16,19–21] SCALMS are composed of bimetallic metal droplets deposited on a porous support material. The bimetallic liquid phase is enriched in a low melting metal, such as Ga, providing the matrix for an atomically dispersed catalytically active transition metal.[16] To date, Rh, Pd, and Pt have been reported for the SCALMS catalyzed dehydrogenation of light alkanes.[13,14,16,17,22,23] While dilution of this active species in the low melting metal increases the melting point when compared to the pure low melting metal, the reaction temperatures may exceed the liquidus temperatures ensuring fully liquid-supported alloys under reaction conditions. SCALMS materials are characterized by a highly dynamic liquid metal–gas interface, which has been proposed as a cyclic movement of the dissolved catalytically active metal atoms to the interface and back into the bulk of the metallic droplet.[14,16] Primarily, this is a result of the thermodynamically favored depletion of the outer layer in this secondary atom, while the adsorption of molecules from the gas phase represents the driving force for the proposed atomic motion. Such a cyclic regeneration of these highly dynamic single-atom sites has been linked to an increased resistance against coking.[13,14,16–18,23] In particular, the rapid desorption of the formed alkene with the subsequent inaccessibility of the active site (due to its movement into the bulk) suppresses coking by hindering the further dehydrogenation of the desired product. Similar dynamic configurations of metallic atoms in the liquid state with critical alignments of reactants and metal atoms enabling an alternative reaction mechanism were also studied by means of computational approaches.[24] Despite this highly dynamic liquid metal–gas interface, SCALMS were also demonstrated to experience deactivation over time during PDH, which may in part be due to a low level of coking.[13,17] Here, the first studies provide strong indications toward a dominant role of the support material in the formation of coke, which may be independent of the catalytic conversion of propane over the supported liquid alloy.[13,17] In particular, acidic sites on the support material are believed to contribute to coking by cracking of formed propylene. This was demonstrated in a previous study comparing Ga-Pt SCALMS with a weakly acidic Al_2O_3 and less functionalized SiO_2 support material.[17] Here, cracking products, such as ethylene and methane, were detected with increasing concentration along the axial direction of the catalyst bed.

Herein, we employ In-Pt SCALMS for PDH using differently functionalized Al_2O_3 supports. Contrary to previous studies, In-based SCALMS can be prepared via simple wet impregnation with subsequent reduction using H_2. To verify the hypothesis that SCALMS generally suppresses coke formation during PDH and that observed minor coking is due to acidic sites on the support material,[17,23] the performance and the coking behavior of In-Pt SCALMS catalysts on Al_2O_3 with different acidity was compared. Performance tests are supported by in situ X-ray diffraction (XRD) and in situ high-resolution thermogravimetric analysis coupled with mass spectrometry (HRTGA-MS).

2. Experimental Section

2.1. Materials

Three types of activated alumina (Al_2O_3) materials (Alfa Aesar, Brockmann Grade I, 80–250 µm particle size) were employed as catalyst supports exhibiting a variety of surface acidity degree from modification by the manufacturer: basic (b-Al_2O_3, lot no. W16F011), neutral (n-Al_2O_3, lot no. P26F029), and acidic (a-Al_2O_3, lot no. 61,800,079).[25–27] All three Al_2O_3 materials were calcined in a muffle furnace at 300 °C for 12 h under a flow of 60 mL_N min^{-1} of synthetic air and stored under static air in a drying oven at 120 °C. The metal precursors $In(NO_3)_3 \bullet xH_2O$ (purity ≥ 99.999%, stock no. 10,708) and $Pt(NH_3)_4(NO_3)_2$ (purity ≥ 99.99%, stock no. 43,897) were purchased from Alfa Aesar. Ethanol (96% purity) and isopropanol (99.8% purity) were purchased from Jäckle Chemie (Germany). All chemicals were used without further purification, dissolved in Millipore water yielding aqueous stock solutions (3.484 mol_{In} L^{-1} and 0.205 mol_{Pt} mL^{-1}), and stored in a refrigerator at 6 °C protected from light.

2.2. Catalyst Preparation

The parent SCALMS catalysts and reference samples were prepared via wet impregnation of the Al_2O_3 support materials. In a typical synthesis, 5.000 g of Al_2O_3 were mixed with aqueous precursor solutions and ethanol in a round bottom flask for rotary evaporators. The precursor solution with a constant fraction of 32 vol.% water in ethanol was composed of one or both aqueous stock solution(s), ethanol, and Millipore water (Table 1) targeting In and Pt loadings of 5.00 and 0.12 wt.%, respectively. After mixing the solid and solution by means of ultrasonication for 5 min, the flask was attached to a rotary evaporator and continuously mixed at 100 rpm and 700 mbar at room temperature to ensure the replacement of air in the pores of the support material by the precursor solution. After 1 h, the temperature was increased to 60 °C using an oil bath and the pressure was reduced to 250 mbar. Afterward, the pressure was reduced in increments of 50–100 mbar and subsequently in increments of 25 mbar to the final pressure of 25 mbar, each pressure level is maintained for 0.5 h. The dry powder was collected and stored overnight in a crucible in a drying oven at 60 °C. Finally, calcination was conducted in a muffle furnace at 500 °C (2 °C min^{-1}) for 3 h with 60 mL_N min^{-1} of synthetic air.

2.3. Catalyst Characterization

The In and Pt loading and the corresponding In/Pt ratios of the SCALMS were determined by inductively coupled plasma atomic emission spectroscopy (ICP-AES) using a Ciros CCD (Spectro Analytical Instruments GmbH). The solid samples were digested in a 3:1:1 volumetric ratio of concentrated HCl:HNO_3:HF using microwave heating up to 220 °C for 40 min. The instrument was calibrated with standard solutions of In and Pt prior to the measurements.

The BET surface area and BJH pore volume of the Al_2O_3 support materials and as prepared SCALMS were analyzed by N_2 physisorption in a QUADROSORB SI surface area and pore size analyzer (Quantachrome Instruments) with a degassing temperature of 200 °C.

CO_2 TPD was performed using a Thermo Scientific TPDRO 1100 instrument equipped with a TCD sensor. An amount of ≈300 mg of material was weighed and dried at 500 °C under helium flow. The sample was cooled to 40 °C and exposed to the sorbent CO_2 for a duration of 60 min and subsequently purged with helium for 15 min.

Table 1. Composition of the precursor solutions for the preparation of the catalysts.

Metals	Support	Al_2O_3	$In(NO_3)_3 \bullet xH_2O$ $_{(aq)}$	$Pt(NH_3)_4(NO_3)_2$ $_{(aq)}$	Ethanol	Water
		g	mmol	mmol	mL	mL
In-Pt	a-Al_2O_3	5.000	2.177	0.0308	6.197	2.030
In-Pt	n-Al_2O_3					
In-Pt	b-Al_2O_3					
In	a-Al_2O_3	5.000	2.177	–	6.197	2.030
In	n-Al_2O_3					
In	b-Al_2O_3					
Pt	a-Al_2O_3	5.000	–	0.0513	6.197	2.030

The TPD data were obtained in a temperature range of 40–650 °C using a heating rate of 10 °C min^{-1}.

NH_3 TPD was performed using a Micromeritics Autochem II instrument equipped with a TCD sensor. An amount of ≈100 mg of material was weighed and dried at 440 °C under helium flow (10 K min^{-1} and 0.5 h holding time). The sample was cooled to 100 °C and exposed to the 10% NH_3/He for a duration of 60 min and subsequently purged with helium for 60 min. The TPD data were obtained in a temperature range of 30–800 °C using a heating rate of 10 K min^{-1} with a 30 min holding time at the final temperature.

X-ray diffraction (XRD) was conducted using an X'Pert PRO (Philipps) equipped with a Cu anode ($\lambda_{K\alpha 1}$ = 1.54,056 Å). The samples were placed in a sample holder and analyzed in a continuous scan mode in the 2θ range of 1.992–80.000° with a step size of 0.0167113° and a scan time of 1.11 s per step. XRD patterns were compared to references from the crystallography open database (COD),[28,29] namely γ-Al_2O_3 (COD ID 2,015,530), In (COD ID 1,538,014), In_2O_3 (COD ID 1,010,341), and PtO_2 (COD ID 1,008,935). Diffraction line broadening analysis via the Scherrer equation[30] with correction for the instrumental line broadening and a shape factor of 0.94 was applied to estimate the crystallite size of In_2O_3.

2.4. In Situ Catalyst Characterization

In situ X-ray diffraction (XRD) studies were conducted during H_2 temperature programmed reduction (TPR) using an in-house developed cell.[31] The cell was mounted to a laboratory diffractometer (Bruker D8 Advance) equipped with a molybdenum source ($\lambda_{k\alpha 1}$ = 0.70,932 Å) and a position-sensitive detector (Bruker AXS Vantec) operated at 50 kV and 35 mA. The powder samples were packed into a capillary in between two quartz wool plugs, loaded onto the cell, and exposed to a diluted stream of 10% H_2/N_2 with a total flow rate of 10 mL_N min^{-1}. The temperature was increased from 50 to 450 °C at a rate of 1 °C min^{-1} with a holding time of 1 h. The temperature was then set to 100 °C with a rate of −1 °C min^{-1} and a holding time of 1 h. Throughout the ramps to 450 °C and holding times, a series of XRD scans of 8 min and 19 s with a 1 min and 41 sec delay were collected in the 2θ range of 12°–20° and a step size of 0.012° using an exposure time of 0.2 s per step. Additionally, a long scan of 1 h and 13 min in the 2θ range of 10°–30° and a step size of 0.006° using an exposure time of 1 s per step was collected at 100 °C after the reduction.

In situ, high-resolution thermogravimetric analysis coupled with mass spectrometry (HRTGA-MS) was conducted during PDH using a previously established procedure.[13,17] A XEMIS sorption analyzer (Hiden Isochema)[32] with a resolution of ±0.1 µg was used, which can be operated at temperatures up to 500 °C. Further post-treatment via temperature-programmed oxidation (TPO) was studied in situ. A total of 200 mg of as prepared In-Pt SCALMS or monometallic Pt/a-Al_2O_3 was loaded and dried under a flow of He (100 mL_N min^{-1}; 500 °C for 6 h with a heating ramp of 5 °C min^{-1}). After cool-down to 100 °C, the catalyst was reduced to 50% H_2/He (overall flow rate: 100 mL_N min^{-1}) in a temperature ramp up to 500 °C at 2 °C min^{-1} with a holding time of 6 h. The system was flushed by He followed by PDH at 500 °C for 24 h using a feed gas composition of 15% C_3H_8/He (overall flow rate: 100 mL_N min^{-1}). The last experimental step during analysis by HRTGA-MS was TPO using 21% O_2/He (overall flow rate: 100 mL_N min^{-1}),[13,17] which was introduced after cool-down to 100 °C under He. TPO was conducted after an initial stabilisation time of 0.5 h at 100 °C during a ramp to 500 °C at 1 °C min^{-1} with a subsequent isotherm at 500 °C for 6 h. The overall pressure was set to ambient conditions throughout the experiments. A mass spectrometer (MS; Hiden Analytical) continuously analyzed the off-gas in the mass-to-charge (m/z) range of 1–50.

2.5. Computational Methodology

All electronic structure calculations of the liquid surface were performed using the density functional theory (DFT) method implemented in the VASP software.[33] The exchange-correlation energy was computed in the generalized gradient approximation (GGA) using the Perdew–Burke–Ernzerhof (PBE) functional.[34] Plane-wave basic functions and the PAW pseudopotential approach are used in VASP.[35] The simulation cell (13 × 13 × 40 Å) contained a slab of $In_{158}Pt_2$ with a thickness of 26.5 Å (Figure S1). To ensure the convergence of the calculations, the energy cut-off was set to 300 eV and the k-point mesh to 2 × 2 × 1. To cancel interactions between replicas of the calculation cell, a vacuum value of over 10 Å was specified. Due to the extremely low concentration of Pt atoms in liquid In (1:79), obtaining reliable statistics on the distribution of particles in the system requires a fairly long molecular dynamics (MD) trajectory. In order to perform this task, we used the machine learning force field (MLFF)[36] approach to parameterize the potential energy calculated from PBE, reducing the computational cost by about three orders of magnitude. In the molecular dynamics simulations, the Nosé-Hoover thermostat[37] with a step of 10 fs at a temperature of 773 K was used. The process of training the force field was first done using an In_{160} system, followed by training on the $In_{158}Pt_2$ system (Figure S1). More details are given in the supporting information (sections MLFF training, Coordination number (CN) analysis, Desorption energy of propylene, as well as Figures S2–S4). The final force field had an energy error of 1.3 meV per atom. The length of the productive run trajectory is 100 ns.

Table 2. Morphology and surface chemistry of the commercial alumina supports.

Support	pH[a]	BET Surface Area / $m^2\ g^{-1}$	BJH Pore Volume / $cm^3\ g^{-1}$
a-Al_2O_3	4.64	145	0.30
n-Al_2O_3	6.95	173	0.34
b-Al_2O_3	9.99	191	0.32

[a] pH of a 10% aqueous slurry.[25–27]

2.6. Propane Dehydrogenation (PDH) in a Fixed Bed Tubular Reactor

The as-prepared catalysts were tested in the propane dehydrogenation reaction in a continuous flow laboratory set-up (Figure S5).[14,23] A total of 1.22 g of the catalyst was placed into the tubular reactor (quartz glass of length 650 mm and inner diameter of 10 mm) that was positioned inside an electrically heated tubular split furnace (Carbolite). The reactor was heated to 500 °C at 10 °C min^{-1} under a flow of 100 $mL_N\ min^{-1}$ of 50% H_2/He for an initial reduction of the parent oxidic catalysts. After 6 h, the reactor was flushed with 100 $mL_N\ min^{-1}$ of He before introducing 8.9 $mL_N\ min^{-1}$ propane (99.95% purity, Linde Gas) as reactant diluted in 89 $mL_N\ min^{-1}$ helium (99.996% purity, Linde Gas). PDH was conducted for 15 h and followed by cool-down under a flow of 100 $mL_N\ min^{-1}$ He. The product stream was analyzed on-line by means of gas chromatography (GC) using a Bruker 456 GC equipped with a GC-Gaspro column (30 m x 0.320 mm) and a flame ionization detector (FID). Mole fractions of compound (x_i) were calculated from peak areas and calibration factors, which were determined for every substance. The conversion of propane (X_{C3H8}), selectivity toward propylene (S_{C3H6}), and the Pt-based productivity toward propylene (P_{C3H6}) were calculated according to Equations 2–4.

$$X_{C3H8} = \frac{x_{C3H8,in} - x_{C3H8}}{x_{C3H8,in}} \cdot 100\% \quad (2)$$

$$S_{C3H6} = \frac{x_{C3H6}}{x_{C3H8,in} - x_{C3H8}} \cdot 100\% \quad (3)$$

$$P_{C3H6} = \frac{\dot{n}_{C3H8,in} \cdot (X_{C3H8}/100\%) \,.\, (S_{C3H6}/100\%) \,.MW_{C3H6}}{m_{Pt}} \quad (4)$$

where $x_{i,in}$ is the initial mole fraction of a compound as calculated based on on-line GC analysis, $\dot{n}_{C3H8}$, in is the total molar flowrate of propane in the feed, MW_{C3H6} is the molar weight of propylene, and m_{Pt} is the overall mass of Pt in the reactor.

3. Results and Discussion

The commercially available support materials with different pH values of aqueous slurries[25–27] (Table 2) were characterized by means of N_2 physisorption (Figure S6) and TPD (Figure S7) to assess the morphology and describe surface functionalization, respectively. The BET surface area increases alongside the pH of an aqueous slurry (Table 2), while BJH analysis suggests comparable specific pore volumes for the differently treated support materials. The surface functionalization by the manufacturer has been confirmed indicating an increase in the number of basic sites in the order a-Al_2O_3 < n-Al_2O_3 < b-Al_2O_3 (a: acidic; n: neutral; b: basic) and an inverse order regarding acidic sites (Figure S6).

Table 3. Metal loadings with molar metal ratio and the corresponding liquidus temperature for the parent catalysts.

Catalyst	In Loading	Pt Loading	In:Pt	Liquidus Temperature[a]
	wt.%	wt.%	mol:mol	°C
$In_{75}Pt/a\text{-}Al_2O_3$	4.82	0.11	75	~210
$In_{78}Pt/n\text{-}Al_2O_3$	4.96	0.11	78	~210
$In_{76}Pt/b\text{-}Al_2O_3$	4.68	0.10	76	~210
$In/a\text{-}Al_2O_3$	5.28	–	–	157
$In/n\text{-}Al_2O_3$	5.15	–	–	157
$In/b\text{-}Al_2O_3$	5.18	–	–	157
$Pt/a\text{-}Al_2O_3$	–	0.18	–	1769

[a] According to the binary Pt-In phase diagram by Okamoto.[38]

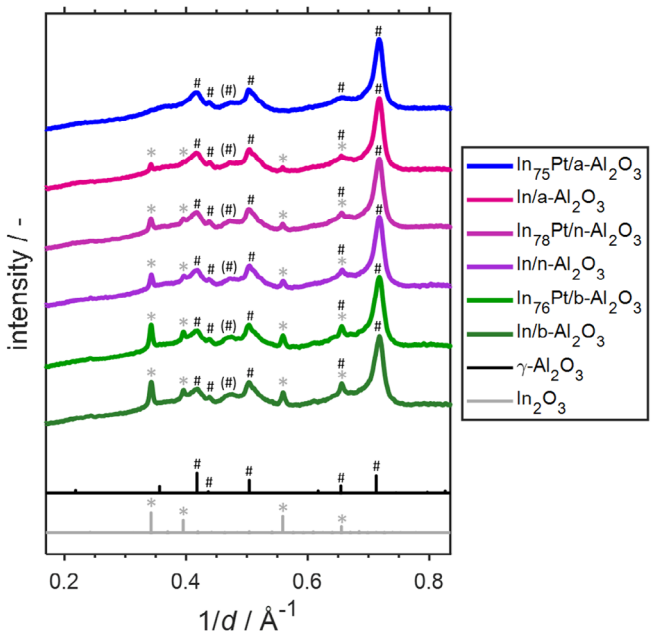

Figure 1. X-ray diffractograms of the parent In-Pt SCALMS catalysts and parent In/Al_2O_3 reference catalysts with differently functionalized support materials, as well as references patterns for In_2O_3 and γ-Al_2O_3.

In-Pt SCALMS were prepared via wet impregnation of the support materials. ICP-AES analyzes of the prepared catalysts after calcination suggest In loadings in the range of 4.7–5.0 wt.% for the surface functionalised support materials (Table 3). Together with Pt loadings of approx. 0.1 wt.%, similar molar ratios of In:Pt in the range of 75–78 were obtained ($In_{75}Pt/a\text{-}Al_2O_3$, $In_{78}Pt/n\text{-}Al_2O_3$, and $In_{76}Pt/b\text{-}Al_2O_3$). The high In content ensures a low melting point of the alloys formed after the reduction of the parent catalysts in H_2 due to the low melting point of In of 157 °C. For the obtained compositions with a Pt content of ≈1.3 mol.%, a fully liquid alloy can be expected at temperatures exceeding 210 °C based on the binary Pt-In phase diagram.[38]

XRD analysis of the calcined catalysts reveals a strong dependence of the In_2O_3 phase on the support materials (Figure 1).

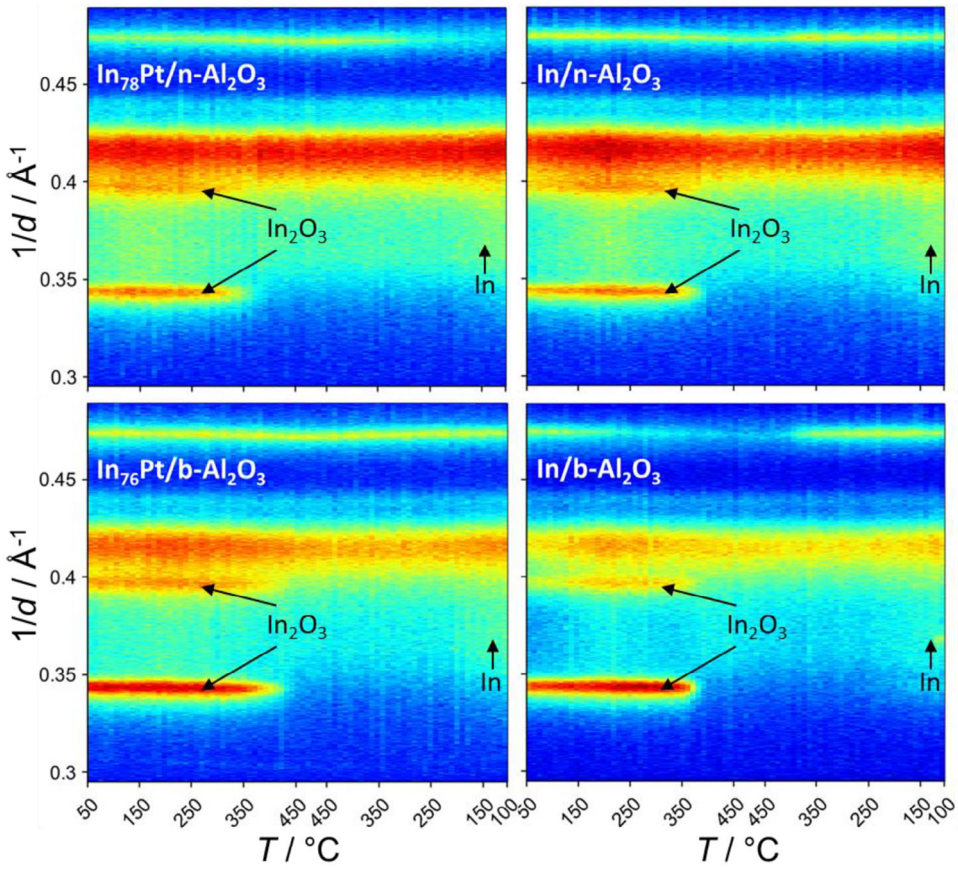

Figure 2. In situ X-ray diffractograms during reduction of a) $In_{78}Pt/n\text{-}Al_2O_3$ SCALMS and b) $In/n\text{-}Al_2O_3$ reference, as well as c) $In_{76}Pt/b\text{-}Al_2O_3$SCALMS and d) $In/b\text{-}Al_2O_3$ reference.

Even though the In loadings are comparable (Table 3), the (222) reflection of In_2O_3 is more and more overlaid by the pattern of the support with increasing acidity of the functionalized support materials. In the case of $In_{75}Pt/a\text{-}Al_2O_3$, the reflections of In_2O_3 are not detectable and the diffraction pattern resembles the bare $a\text{-}Al_2O_3$ support material (Figure S8). For the supports, only a reflection at 0.47 $Å^{-1}$, which is highlighted with (#), is not matched by the $\gamma\text{-}Al_2O_3$ reference but is present in all diffractograms (Figure S8). A similar observation was made for reference In/Al_2O_3 catalysts, which were prepared in the same manner by impregnation of the three surface functionalized supports without a Pt precursor (Figure 1). Here, the maximum intensity of the (222) reflection decreases with the acidity as well, but remains detectable in the pattern of the $In/a\text{-}Al_2O_3$ reference. Scherrer diffraction line broadening analysis was conducted to approximate the crystallite size of the In_2O_3 phases. An average size of 19 nm was obtained for both In-Pt catalysts ($n\text{-}Al_2O_3$ and $b\text{-}Al_2O_3$), while an average size of 17, 21, and 26 nm ($In/a\text{-}Al_2O_3$) were identified for the monometallic reference catalysts. Even though the analysis is affected by the undefined diffraction line broadenings of the $\gamma\text{-}Al_2O_3$ supports, this observation suggests the formation of differently sized crystallographic domains in the metal oxides. In accordance with the low loadings of Pt (Table 3), no reflections of Pt or PtO_x can be identified.

Reductive treatment of the catalysts in H_2 is expected to transform the parent oxide phase into a liquid, In-rich metal on the alumina support yielding SCALMS. H_2 TPR of the catalysts was combined with in situ XRD to monitor the reduction process of the dominant In_2O_3 phase at elevated temperatures (Figure 2). As no In_2O_3 reflections could be detected in the $a\text{-}Al_2O_3$-supported parent catalyst (Figures 1 and S9), the reduction may only be tracked for the other catalysts. For $In_{78}Pt/n\text{-}Al_2O_3$, the In_2O_3 reflections reduce in intensity at a temperature range of 270–400 °C due to the reduction to metallic liquid In. Reduction of In_2O_3 in H_2 atmosphere has been reported at temperatures exceeding 300 °C,[39,40] which is also evidenced by the $In/n\text{-}Al_2O_3$ reference with reduction temperatures of 320–370 °C. Hence, the lower reduction temperature of the $In_{78}Pt/n\text{-}Al_2O_3$ catalyst may be linked to the initial reduction of PtO_x with subsequent H_2-spillover to the In_2O_3 phase, which has been reported for Ga-Pt SCALMS.[17,23] However, the opposite behavior was observed for the $b\text{-}Al_2O_3$-supported catalyst with reduction of $In_{76}Pt/b\text{-}Al_2O_3$ SCALMS at 440 and 400 °C for the $In/b\text{-}Al_2O_3$ reference. As expected, no phases other than the support are detected at the maximum reduction temperature of 450 °C for all catalysts due to the liquid nature of the metal (solutions). Lastly, the cool-down of the catalysts under H_2 atmosphere was also monitored. A weak reflection for metallic In was detectable at 0.37 $Å^{-1}$ for all catalysts below approx. 200 °C, which is just below the melting point of pure In and hence is linked to the

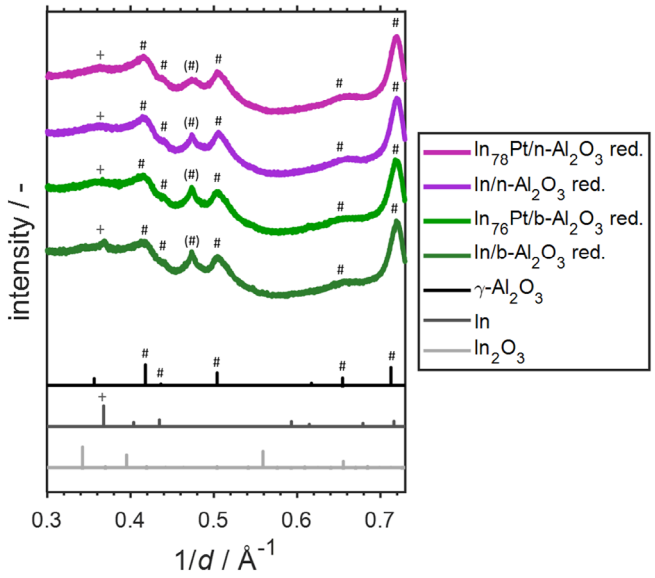

Figure 3. X-ray diffractograms of the In-Pt SCALMS and monometallic In references using n-Al_2O_3 and b-Al_2O_3 supports after in situ reduction in H_2 with reference patterns of the supports as well as In and In_2O_3.

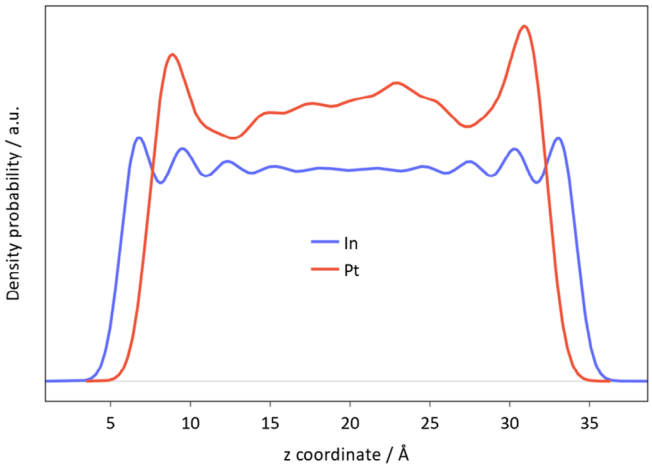

Figure 4. The density distribution function of particle detection relative to the direction orthogonal to the plane of the liquid surface for $In_{158}Pt_2$ as obtained from a 100 ns MLFF-MD run.

solidification of the liquid metal (alloy). The final patterns after cool-down were then compared to the parent catalysts (Figures 3 and S9) confirming the absence of detectable In_2O_3 reflections. Most reduced catalysts have an increased intensity at 0.37 $Å^{-1}$, which suggests an undefined contribution of metallic In to the patterns. This may be related to amorphous In in consequence of the presence of Pt in the alloy and/or the surface functionalization of the supports. For the In/b-Al_2O_3 reference catalyst, even a defined peak for metallic In is detectable.

The use of indium as a metal with a low melting point enables the presented approach for preparing SCALMS via a simplified wet impregnation approach. Previously applied Ga-based SCALMS were dominantly prepared via decomposition of an organometallic Ga precursor[16] or ultrasonication of liquid gallium,[23] followed by galvanic displacement as oxide phases must be avoided due to the low reducibility of Ga_2O_3 in combination with a high vapor pressure of gallium oxide species.[18,41] This facilitated preparation comes along an improved resource efficiency and scalability. Hence, In-based SCALMS may have an even bigger impact with respect to technical application. However, a maximum capacity for the In loading was identified in preliminary studies. Here, phase separation between the support and liquid In was observed after the reduction of the catalyst with an In loading of 18.1 wt.% in H_2 (Figure S10).

We performed MLFF-MD simulations to investigate the Pt location within In using a In:Pt ratio of 79:1 similar to the herein prepared In-Pt SCALMS. The surface of In (first 2–3 layers) is somewhat ordered such that surface and subsurface peaks of In are visible (Figure 4). Pt is located within the liquid, but has a notable subsurface presence. This is in line with previously published ab initio simulations on similar liquid alloys, namely Ga-rich Ga-Pd,[16] Ga-Rh,[14] and Ga-Ni.[18] This enrichment of the noble metals below the In-rich surface enables the dynamic formation of active sites whenever Pt pops up to the surface due to potential interaction with the reactant.[19] In our case and based on the statistical evaluation of MLFF-MD simulations, about 0.53% of the In surface contains Pt. We also approximated the frequency of Pt being at the surface of the liquid $In_{158}Pt_2$. There is a small probability of Pt exhibiting a coordination number of 6 while being close to the surface (once per 42.25 ps, Figure S4). Further, the calculation of the desorption energy of propylene (see Supporting Information for details) resulted in 0.17 eV, which indicates facile desorption. Hence, blocking of active Pt sites is unlikely.

After demonstration of the general suitability of the In-Pt system as SCALMS by means of in situ XRD to study the transformation of the prepared oxidic parent catalysts into supported liquid metals and theoretical studies of liquid In-Pt alloys, PDH was conducted in a fixed-bed reactor at 500 °C for 15 h (Figure 5). Both, the $In_{75}Pt$/a-Al_2O_3 and $In_{78}Pt$/n-Al_2O_3 SCALMS exhibit an almost constant conversion of propane between 5.0% and 6.2% throughout the experiment (Figure S11). Typically, Pt-based catalysts suffer from rapid deactivation requiring frequent regeneration treatments.[9,14,17,23] The $In_{76}Pt$/b-Al_2O_3 catalyst outperformed the other SCALMS with initial conversion beyond 10%, but displayed a more pronounced deactivation. Interestingly, the similar performance after 15 h time on stream (TOS) suggests similar morphological properties of the three SCALMS, i.e., rearrangement of $In_{76}Pt$/b-Al_2O_3 catalyst seemingly diminishes the initial beneficial state. The exact origin of this different catalytic performance remains unclear, but may be linked to droplet size, residual oxidic phases or surface acidity. An In/n-Al_2O_3 benchmark did not show significant activity toward PDH after in situ reduction in H_2 (Figure S12), which in turn points toward the activity of SCALMS due to the introduction of Pt.

The productivity of the SCALMS is comparable to previously reported Ga-Pt SCALMS, while the $In_{76}Pt$/b-Al_2O_3 exhibits the best performance of all Pt-based SCALMS to date (Table 4). Only a Ga-Rh SCALMS exceeded the productivity of this catalyst, but at the expense of a lower propylene selectivity. All SCALMS led to a similarly high (gas phase) selectivity toward propylene

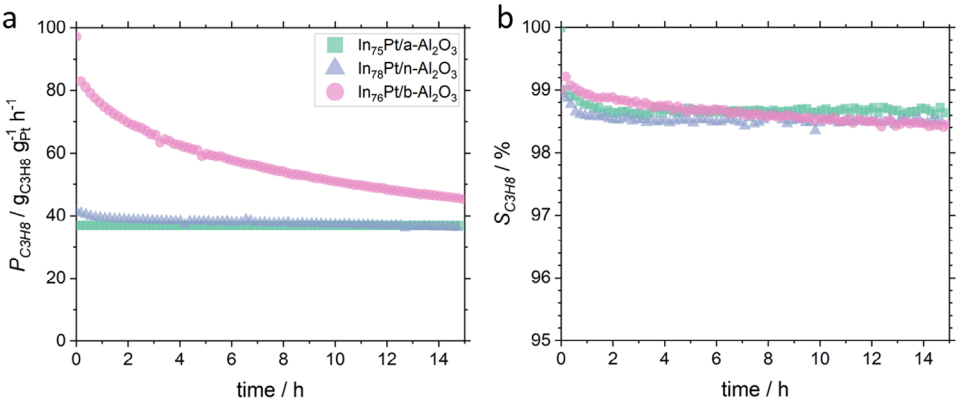

Figure 5. a) Platinum-based productivity and b) selectivity towards propylene during non-oxidative dehydrogenation of propane over In-Pt SCALMS. Conditions of the experiment: 500 °C; 89 mL_N min^{-1} He; 8.9 mL_N min^{-1} C_3H_8; WHSV 4815 mL_N g^{-1} h^{-1}.

Table 4. Key performance indicators of the In-Pt SCALMS in this study compared to related Ga-based SCALMS.

Catalyst	Reference	In / Ga	Pt / Rh	$P_{C3H6,0h}$*	$P_{C3H6,14h}$*	$S_{C3H6,14h}$*
		wt.%	wt.%	g_{C3H6} $g_{Pt/Rh}^{-1}$ h^{-1}	g_{C3H6} $g_{Pt/Rh}^{-1}$ h^{-1}	$\%_{C3H6}$
$In_{75}Pt/a\text{-}Al_2O_3$	This study	4.82	0.11	37	37	98.6
$In_{78}Pt/n\text{-}Al_2O_3$	This study	4.96	0.11	42	36	98.4
$In_{76}Pt/b\text{-}Al_2O_3$	This study	4.68	0.10	83	45	98.4
$Ga_{49}Pt/Al_2O_3$	[23]	2.11	0.12	44	22	99.5
$Ga_{89}Rh/Al_2O_3$	[14]	6.06	0.10	92	52	92.0

*Productivity and selectivity after 0 or 14 h TOS with comparable propane conversion levels after 14 h TOS in the range of 3.8% to 7.1%.

of >98.5% throughout the 15 h TOS, which does not include the share of solid or condensable coking products. Organic residues were detected at the unheated reactor outlet for the a-Al_2O_3 and n-Al_2O_3 supported catalysts (Figure S13), which suggests a certain level of coking for both SCALMS. No metals were detected during the analysis of the residues. Coke formation may impede catalyst activity if blocking active sites. Dedicated in situ studies were performed to quantify the amount of carbon deposits on the catalyst and to provide insight into the formation of gaseous by-products from coking.

In situ HRTGA-MS was conducted during PDH after activation in H_2. The procedure was similar to reported studies using Ga-Pt SCALMS with metal oxide and SiC support materials.[13,17,23] Comparison of the relative sample weight over TOS of $In_{75}Pt/a\text{-}Al_2O_3$ SCALMS with a $Pt/a\text{-}Al_2O_3$ benchmark catalyst (Figure 6a) demonstrates the general benefit of the SCALMS concept to suppress coking to a certain extent.[13,14,17,18,23] A more than twofold increase in the sample weight was observed for the benchmark when compared to the SCALMS. The weight increase can be mostly assigned to coking,[17] which is supported by an enhanced H_2 formation as indicated by the continuously high intensity of the m/z ratio of 2 (Figure 6b). Aside from PDH, H_2 is also a main product of coking. The difference in coke formation between $In_{75}Pt/a\text{-}Al_2O_3$ SCALMS and $Pt/a\text{-}Al_2O_3$ can be mostly assigned to the presence of monometallic Pt clusters in the latter, as both catalysts have the same support. Comparison of the different SCALMS reveals a dependence of the formation of carbon deposits on the surface acidity of the support. Here, the relative weight increases, as expected, with increasing acidity. Interestingly, the relative weight increases in a linear manner for the $In_{75}Pt/a\text{-}Al_2O_3$ and $In_{78}Pt/n\text{-}Al_2O_3$ SCALMS, while a plateau is observed for the weight increase of $In_{76}Pt/b\text{-}Al_2O_3$ suggesting mostly initial coke formation in the first 20 h TOS (Figure 6a).

The carbon deposits on the catalysts were subsequently oxidized during TPO in a continuation of the in situ HRTGA-MS based on previously developed protocols (Figure 7).[13,17] First exposure of the reduced catalysts to the oxidizing agent O_2 results in a mass increase in the SALMS due to (surface) oxidation of indium.[17] Here, the suggested dependence of the amount of coke on the support acidity is confirmed with the highest amount (3.5 wt.%) for the $Pt/a\text{-}Al_2O_3$ reference followed by the SCALMS with decreasing acidity ($In_{75}Pt/a\text{-}Al_2O_3$: 1.9 wt.%; $In_{78}Pt/n\text{-}Al_2O_3$: 0.6 wt.%; $In_{76}Pt/b\text{-}Al_2O_3$: 0.2 wt.%). The authors note that the initial weight increase due to oxidation of In (and Pt) strongly affects the quantification of coke. Qualitative analysis of the formation of CO_2 suggests a similar type of carbon deposits for all SCALMS catalysts with maximum formation of CO_2 at approx. 470 °C (Figure 7b), which suggests similar coke compositions as in previous SCALMS.[13,17] Only a more intense CO_2 formation at lower temperatures (350–400 °C) for $In_{75}Pt/a\text{-}Al_2O_3$ suggests an enhanced formation of soft coke on this SCALMS.[13] Carbon deposits in the $Pt/a\text{-}Al_2O_3$ benchmark were less reactive.

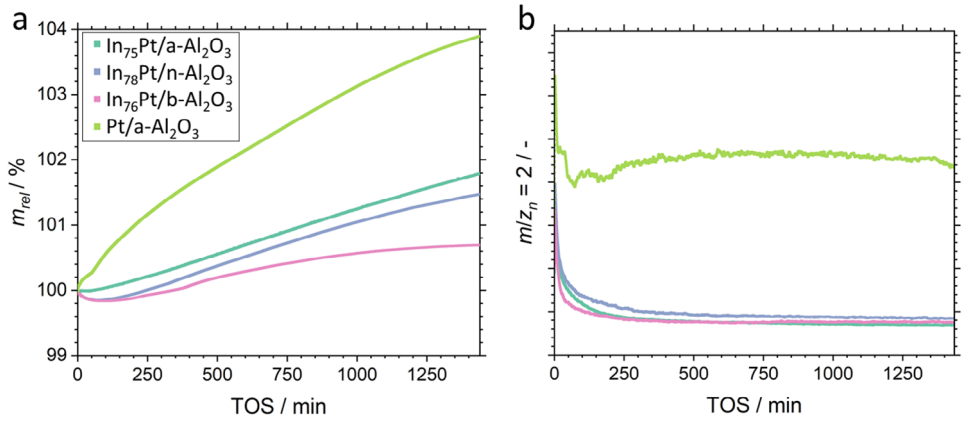

Figure 6. a) Sample weight relative to the weight of the dried catalyst during propane dehydrogenation over In-Pt SCALMS with surface-modified Al_2O_3 support materials and a supported Pt reference sample with b) mass-to-charge ratio of 2 representing almost exclusively H_2 as monitored via in situ high-resolution thermogravimetry coupled with mass spectrometry. Conditions of the experiment: 500 °C; 85 mL_N min^{-1} He; 15 mL_N min^{-1} C_3H_8; WHSV 30,000 mL_N g^{-1} h^{-1}.

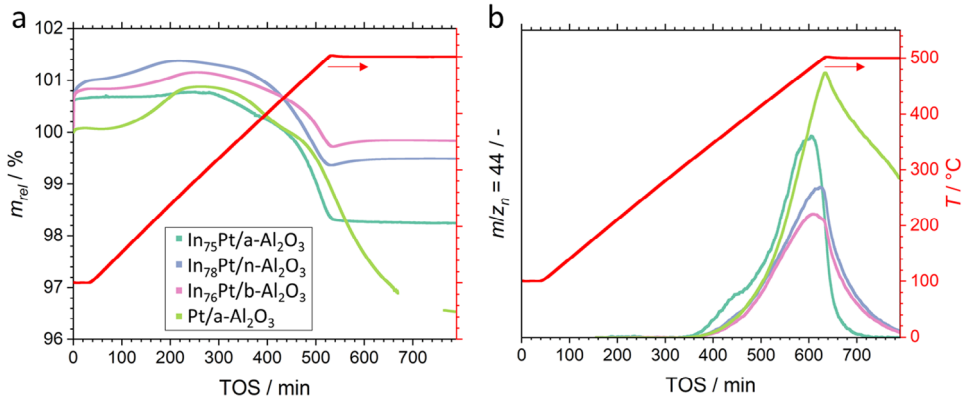

Figure 7. a) Sample weight relative to the catalyst weight after propane dehydrogenation over In-Pt SCALMS with surface-modified Al_2O_3 support materials and a supported Pt reference sample during temperature programmed oxidation with b) mass-to-charge ratio of 44 representing CO_2 as monitored via in situ high-resolution thermogravimetry coupled with mass spectrometry. Conditions of the experiment: 80 mL_N min^{-1} He; 20 mL_N min^{-1} O_2; WHSV 30,000 mL_N g^{-1} h^{-1}.

Overall, the comparison of In-Pt SCALMS using differently functionalised Al_2O_3 supports demonstrates the previously hypothesized dominating role of the support on coking when using SCALMS in PDH.[17,23] Even though a more than twofold increase in coke formation was quantified for the a-Al_2O_3 when compared to the basic support (Figures 6 and 7), the catalytic activity was seemingly not altered regardless of coking being a common driver for catalyst deactivation. The three SCALMS rather demonstrate an equilibration independent of support functionalization during PDH resulting in similar productivities after a run-in phase (Figure 5). Hence, the initial differences in the dehydrogenation activity is seemingly related to a strong dependence of the morphology of the parent metal oxide on the surface acidity of the Al_2O_3 support as evidenced by XRD (Figure 1). Larger metal oxide crystallite sizes, as suggested by a stronger peak intensity in XRD for the parent $In_{76}Pt/b\text{-}Al_2O_3$ catalyst, suggest weaker interaction of the metal oxide with basic sites, which potentially results in the formation of larger liquid droplets. Redispersion of this liquid phase during PDH may result in similar droplet sizes and hence an activity similar to the other two SCALMS. In addition, the potential contribution of residual metal oxides to coking and, more importantly, the observed PDH activity remains unclear. Mixed indium oxides have been reported to catalyze PDH.[42] The amount of residual oxide species upon reduction and during PDH may also depend on the support functionalization and initial morphology of the metal oxide in the parent catalyst. This effect will be studied in future work, which will focus on the effect of different In:Pt ratios. As demonstrated, the presence of Pt strongly affects the overall reducibility of the metal oxides. Hence, the Pt concentration may be used as a modulator for residual metal oxide species in the catalysts. However, the contribution of such metal oxide species may be limited as the In/n-Al2O3 benchmark did not show significant activity during PDH.

4. Summary and Conclusion

The influence of surface acidity on the preparation, reductive activation, and activity during non-oxidative propane dehydro-

genation was studied using Al_2O_3 supported In-Pt liquid alloys according to the SCALMS concept. The use of acidic, neutral, and basic Al_2O_3 supports strongly affected the resulting In_2O_3 structure after calcination, which was most prominent in XRD for the basic-modified support after calcination even though the loadings were comparable for all catalysts. In situ reduction of the parent catalysts resulted in a supported liquid alloy rendering the catalysts SCALMS. The good reducibility of In_2O_3 enables this simplified approach for the preparation of SCALMS, which cannot be applied to Ga-based SCALMS from previous studies. In accordance with literature focussing on Ga-based SCALMS, molecular dynamics simulation suggests an enrichment of Pt below the surface of the In-rich liquid alloy. The SCALMS with basic-modified Al_2O_3 outperformed the other catalysts during propane dehydrogenation and was most resistant against coking. The SCALMS with more acidic supports showed a stable conversion even though in situ high-resolution thermogravimetric analysis identified a more pronounced continuous build-up of coke than for a basic modification. Hence, the coking of SCALMS is seemingly dominated by the support as previously hypothesized. In conclusion, coke formation as such has a seemingly limited effect on the catalytic activity of SCALMS. A Pt/Al_2O_3 benchmark using the acidic modification resulted in vast coking exemplifying the high coking resistance of SCALMS.

Acknowledgements

Financial support by the European Research Council (Project 786475: Engineering of Supported Catalytically Active Liquid Metal Solutions), the German Research Foundation (DFG) in the frame of the Collaborative Research Centre 1452 Catalysis at Liquid Interfaces (CLINT), and the Helmholtz Research Program "Materials and Technologies for the Energy Transition (MTET), Topic 3: Chemical Energy Carriers" is gratefully acknowledged. The authors thank Susanne Pachaly for conducting ex situ XRD measurements, Phillip Nathrath for analysis by means of NH_3-TPD at FAU, as well as Fabian Kroll and Ludger Röhm for preparation and testing of the $In/n\text{-}Al_2O_3$ benchmark, respectively.

Open access funding enabled and organized by Projekt DEAL.

Conflict of Interests

The authors declare no conflict of interest.

Data Availability Statement

The data that support the findings of this study are available in the supplementary material of this article.

Keywords: Coking · Dehydrogenation · In situ XRD · Surface functionalization · Thermogravimetry

[1] T. Otroshchenko, G. Jiang, V. A. Kondratenko, U. Rodemerck, E. V. Kondratenko, *Chem. Soc. Rev.* **2021**, *50*, 473–527.
[2] K. J. Caspary, H. Gehrke, M. Heinritz-Adrian, M. Schwefer, in: *Handbook of Heterogeneous Catalysis* (Eds: G. Ertl, H. Knözinger, F. Schüth, J. Weitkamp), Wiley, Weinheim **2008**.
[3] O. O. James, S. Mandal, N. Alele, B. Chowdhury, S. Maity, *Fuel Proc. Technol.* **2016**, *149*, 239–255.
[4] J. S. Plotkin, *Catal. Today* **2005**, *106*, 10–14.
[5] Sattler, J. J. H. B., J. Ruiz-Martinez, E. Santillan-Jimenez, B. M. Weckhuysen, *Chem. Rev.* **2014**, *114*, 10613–10653.
[6] R. D. Cortright, J. M. Hill, J. A. Dumesic, *Catal. Today* **2000**, *55*, 213–223.
[7] H. Lieske, A. Sárkány, J. Völter, *Appl. Catal.* **1987**, *30*, 69–80.
[8] J. M. Hill, R. D. Cortright, J. A. Dumesic, *Appl. Catal. A* **1998**, *168*, 9–21.
[9] Q. Li, Z. Sui, X. Zhou, Y. Zhu, J. Zhou, D. Chen, *Top. Catal.* **2011**, *54*, 888–896.
[10] A. Iglesias-Juez, A. M. Beale, K. Maaijen, T. C. Weng, P. Glatzel, B. M. Weckhuysen, *J. Catal.* **2010**, *276*, 268–279.
[11] H. N. Pham, Sattler, J. J. H. B., B. M. Weckhuysen, A. K. Datye, *ACS Catal.* **2016**, *6*, 2257–2264.
[12] T. Otroshchenko, S. Sokolov, M. Stoyanova, V. A. Kondratenko, U. Rodemerck, D. Linke, E. V. Kondratenko, *Angew. Chem., Int. Ed.* **2015**, *54*, 15880–15883.
[13] M. Wolf, N. Raman, N. Taccardi, M. Haumann, P. Wasserscheid, *ChemCatChem* **2020**, *12*, 1085–1094.
[14] N. Raman, S. Maisel, M. Grabau, N. Taccardi, J. Debuschewitz, M. Wolf, H. Wittkämper, T. Bauer, M. Wu, M. Haumann, C. Papp, A. Görling, E. Spiecker, J. Libuda, H.-P. Steinrück, P. Wasserscheid, *ACS Catal.* **2019**, *9*, 9499–9507.
[15] J. Im, M. Choi, *ACS Catal.* **2016**, *6*, 2819–2826.
[16] N. Taccardi, M. Grabau, J. Debuschewitz, M. Distaso, M. Brandl, R. Hock, F. Maier, C. Papp, J. Erhard, C. Neiss, W. Peukert, A. Görling, H. P. Steinrück, P. Wasserscheid, *Nat. Chem.* **2017**, *9*, 862–867.
[17] M. Wolf, N. Raman, N. Taccardi, R. Horn, M. Haumann, P. Wasserscheid, *Faraday Discuss.* **2021**, *229*, 359–377.
[18] M. Wolf, A. L. de Oliveira, N. Taccardi, S. Maisel, M. Heller, S. Khan Antara, A. Søgaard, P. Felfer, A. Görling, M. Haumann, P. Wasserscheid, *Commun. Chem.* **2023**, *6*, 224.
[19] G. Rupprechter, *Nat. Chem.* **2017**, *9*, 833–834.
[20] J. M. Herman, A. P. A. F. Rocourt, P. J. van den Berg, P. J. van Krugten, J. J. F. Scholten, *Chem. Eng. J.* **1987**, *35*, 83–103.
[21] A. Riisager, R. Fehrmann, M. Haumann, P. Wasserscheid, *Europ. J. Inorg. Chem.* **2006**, *2006*, 695–706.
[22] T. Bauer, S. Maisel, D. Blaumeiser, J. Vecchietti, N. Taccardi, P. Wasserscheid, A. Bonivardi, A. Görling, J. Libuda, *ACS Catal.* **2019**, *9*, 2842–2853.
[23] N. Raman, M. Wolf, M. Heller, N. Heene-Würl, N. Taccardi, M. Haumann, P. Felfer, P. Wasserscheid, *ACS Catal.* **2021**, *11*, 13423–13433.
[24] J. Tang, A. J. Christofferson, J. Sun, Q. Zhai, P. V. Kumar, J. A. Yuwono, M. Tajik, N. Meftahi, J. Tang, L. Dai, G. Mao, S. P. Russo, R. B. Kaner, M. A. Rahim, K. Kalantar-Zadeh, *Nat. Nanotechnol.* **2024**, *19*, 306–310.
[25] ThermoFisher Scientific Certificate of Analysis: Aluminum oxide, activated, neutral, Brockmann Grade I, 58 angstroms **2021**, Product No.: 11502, Lot No.: P26F029.
[26] ThermoFisher Scientific Certificate of Analysis: Aluminum oxide, activated, basic, Brockmann Grade I, 58 angstroms **2021**, Product No.: 11503, Lot No.: W16F011.
[27] ThermoFisher Scientific Certificate of Analysis: Aluminum oxide, activated, acidic, Brockmann Grade I, 58 angstroms **2021**, Product No.: 11501, Lot No.: 61800079.
[28] S. Gražulis, D. Chateigner, R. T. Downs, A. F. T. Yokochi, M. Quirós, L. Lutterotti, E. Manakova, J. Butkus, P. Moeck, A. Le Bail, *J. Appl. Crystallogr.* **2009**, *42*, 726–729.
[29] R. T. Downs, M. Hall-Wallace, *Am. Mineral.* **2003**, *88*, 556-566.
[30] P. Scherrer, *Nachr. Ges. Wiss. Gottingen, Math.-Phys. Kl.* **1918**, 98–100.
[31] N. Fischer, M. Claeys, *Catal. Today* **2016**, *275*, 149–154.
[32] D. L. Minnick, T. Turnaoglu, M. A. Rocha, M. B. Shiflett, *J. Vac. Sci. Technol.* **2018**, *36*, 50801.

[33] G. Kresse, J. Furthmüller, *Phys. Rev. B Condens. Matter.* **1996**, *54*, 11169–11186.
[34] J. P. Perdew, K. Burke, M. Ernzerhof, *Phys. Rev. Lett.* **1996**, *77*, 3865–3868.
[35] G. Kresse, D. Joubert, *Phys. Rev. B Condens. Matter.* **1999**, *59*, 1758–1775.
[36] R. Jinnouchi, J. Lahnsteiner, F. Karsai, G. Kresse, M. Bokdam, *Phys. Rev. Lett.* **2019**, *122*, 225701.
[37] D. J. Evans, B. L. Holian, *J. Chem. Phys.* **1985**, *83*, 4069–4074.
[38] H. Okamoto, *J. Phase Equilib. Diff.* **2014**, *35*, 636–648.
[39] M. Ziemba, L. Schumacher, C. Hess, *J. Phys. Chem. Lett.* **2021**, *12*, 3749–3754.
[40] M. Ziemba, M. Radtke, L. Schumacher, C. Hess, *Angew. Chem., Int. Ed.* **2022**, *61*, e202209388.
[41] T. Terasako, Y. Kawasaki, M. Yagi, *Thin Solid Films* **2016**, *620*, 23–29.
[42] S. Tan, S.-J. Kim, J. S. Moore, Y. Liu, R. S. Dixit, J. G. Pendergast, D. S. Sholl, S. Nair, C. W. Jones, *ChemCatChem* **2016**, *8*, 214–221.

Manuscript received: December 20, 2024
Revised manuscript received: April 12, 2025
Accepted manuscript online: April 12, 2025
Version of record online: May 3, 2025